Supporting Information

Strombach et al. 10.1073/pnas.1414715112

SI Materials and Methods

Additional Analyses. In addition to those presented in the main text, we performed further analyses to explore alternative explanations of TPJ functionality. In particular, we aimed to elaborate on the possibility that the TPJ represents the value attached to increasing another person's well-being.

These analyses were variants of (*i*) the GLMs described in the main text (decision onset split according to generous and selfish decisions), and (*ii*) an additional GLM in which all decision onsets were collapsed into one vector, thus not conditioned by choice.

For the GLM presented in the main text, we used the following parametric modulations for the onset regressor of generous decisions to model other-regarding utilities (ORUs):

a) the amounts foregone at the indifference point;
b) the ORU minus the selfish reward magnitude, thus the relative value of the chosen, generous option;
c) the inverse of the social distance as absolute numerical value;
d) *z* scores of the social distance.

For GLM (*ii*), in which all decisions were collapsed into one vector, we used the following parametric modulations:

e) the ORU in all trials, independent of whether the decision was generous or selfish;
f) the ORU independent of the actual decision as a first parametric modulator, selfish reward magnitude as a second parametric modulator;
g) the selfish reward magnitude as a first parametric modulator, ORU (independent of the actual decision) as a second parametric modulator;
h) the inverse of the social distance as absolute numerical value;
i) the value of the chosen minus the value of the unchosen option, independent of whether the decision was generous or selfish.

None of these contrasts revealed significant activation in the TPJ, even at very liberal thresholds ($P < 0.01$, uncorrected).

Onset of the Second Option. All information necessary to make a decision was already available after presentation of the second option (generous or selfish alternative; see Fig. 1 in main text for details). Thus, it is possible that our participants already integrated all decision-relevant information at this time point, and formed their decision before it was revealed at decision onset. To test this possibility, we modulated the BOLD response at the onset of the second option to estimate the neural response to social discounting in addition to the GLM reported in the main text in which we used the time point of the revealed decision. Because the order of the options was randomized, either the generous or the selfish option was presented second. We estimated the following GLM, consisting of four onset regressors: (*i*) onset of the second option, generous decision; (*ii*) onset of the second option, selfish decision; (*iii*) onset of a generous decision; and (*iv*) onset of a selfish decision. For all four regressors, we included the temptation to be selfish (own-reward value minus ORU) as parametric modulators. We were especially interested in comparing the parametric modulators for onset regressors *i* and *iii* as well as *ii* and *iv* to examine whether we can identify similar activation patterns at the two distinct time points.

A conjunction analysis revealed a significant overlap between the parametric modulation of the temptation to be selfish, given a generous decision at the time of presentation of the second option (onset regressor *i*) and at the time of the revealed decision (onset regressor *iii*; Fig. S2). We find similar patterns also for the temptation to be selfish, given a selfish decision during both onsets.

Thus, the data suggest that similar neural networks were active at onset of the second option and decision onset. However, as it is difficult to isolate decision-making processes from potentially choice-irrelevant sensory or computational processes related to the presentation of the second option, and because the consideration of all relevant choice information is only ultimately evident when a decision is revealed, we decided to report neural activations at decision onset in the main manuscript.

Reaction Times. To control for a possible effect of reaction times on BOLD responses, we performed additional analyses on behavioral and neural data. First, a paired-sample *t* test was carried out to compare the reaction times (time between decision prompt and decision onset) of generous (M = 0.726, SD = 0.226) and selfish decisions (M = 0.731, SD = 0.250). The test did not indicate a significant difference in reaction time (RT) between the two types of decisions [$t_{(22)} = -0.176$, $P = 0.862$; Fig. S3].

Second, to explore the possibility that RTs were correlated with BOLD responses, we included individual reaction times at decision onset as additional parametric modulators in the first GLM reported in the main text. Our aim was to investigate whether activity in the VMPFC might be influenced by variability in reaction times, as VMPFC has been shown to be sensitive to response speed (1–3). Thus, we added two parametric modulators to the GLM in the main text for the regressor for the onset of the selfish decisions: (*i*) the magnitude of the selfish reward and (*ii*) the RT.

Using the same VMPFC ROI as in the manuscript (4), in the correlation between VMPFC-BOLD signal and the selfish reward magnitude at decision onset remained significant [−6, 41, 5; $t_{(22)} = 3.09$, $P = 0.034$] even after controlling for reaction times. Thus, it is unlikely that differences in RTs accounted for VMPFC activity and to conclude that VMPFC activity genuinely reflected the selfish utility.

High vs. Low Other-Regarding Trials. In our experiment, we included generous trial types with high (€75 own-reward/€75 other-reward) and low (€75 own-reward and €25 other-reward) other-reward alternatives. In our main analyses, we pooled across high- and low other-reward trial types for the following reasons.

First, we found no significant differences in neural activation between the low and high other-reward trials anywhere in the brain, including VMPFC and TPJ. More specifically, we used an additional GLM to compare high and low other-reward trials. This GLM contained the following onset regressors: (*i*) onset of the decision, given a high other-reward trial; and (*ii*) onset of the decision, given a low other-reward trial. With an initial threshold of $P < 0.005$, $k \geq 10$ voxel, the contrast between the high and low other-reward regressors revealed no significantly activated voxel anywhere. Also, when using a mask of both the parietal part of rTPJ and the whole rTPJ (5), we found no significant small-volume (SV)–corrected differences in activation (all $P > 0.05$, FWE SV corrected).

Second, we found no differences in activation between the high and low other-reward trials in valuation networks, including the VMPFC: using a 6-mm sphere around the VMPFC-ROI identified in a metaanalysis (−2, 40, −4; ref. 4), which was also used in the main analysis, revealed no significant activation after SV correction ($P > 0.05$, FWE SV corrected).

Third, in a further analysis, we investigated whether TPJ, in particular, was differentially activated in high and low other-reward trials given a generous decision. To this end, we calculated an additional GLM with one onset regressor for low other-reward trials, given a generous decision and one onset regressor for high other-reward trials, given a generous decision. Neither a whole-brain analysis ($P > 0.005$, uncorrected) nor a SV correction using the mask from Mars et al. (5) revealed any significant difference between high and low other-regarding trials in the TPJ.

Because these analyses revealed no meaningful difference in neural activity between high and low other-reward trials, and to preserve statistical power, we pooled across high and low other-reward trial types in our main analyses.

Social Distance or General Metric of Magnitude? It is possible that the participants may not have been considering social distance during the task but rather a more general metric of magnitude or distance. However, we think it is unlikely that our participants disregarded the social nature of the distance scale. This is evident from the participants' behavior. Our results showed that participants were always less generous toward recipients at remote compared with close social distances. Our participants would not have shown this decrease in generosity across social distance had they disregarded social distance. It is important to highlight that the experiment was carried out in an incentive-compatible manner and that subjects were asked to indicate representatives for several social distances (including name and their relationship to that person). Therefore, we assume that subjects were aware of the fact that their decisions could affect the well-being of another person. Moreover, if the TPJ was only processing a general numeric metric of social distance, independent of its social significance, TPJ activation should have been unmodulated by the type of decision (selfish/generous), but this is not what we found. Our results showed that TPJ activity was higher for generous vs. selfish decisions (see main text), although the numerical metric of social distance was identical in both generous and selfish decisions.

1. Büchel C, Holmes AP, Rees G, Friston KJ (1998) Characterizing stimulus-response functions using nonlinear regressors in parametric fMRI experiments. *Neuroimage* 8(2):140–148.
2. Frackowiak RS, et al. (2004) *Human Brain Function* (Academic, London).
3. Grinband J, Wager TD, Lindquist M, Ferrera VP, Hirsch J (2008) Detection of time-varying signals in event-related fMRI designs. *Neuroimage* 43(3):509–520.
4. Clithero JA, Rangel A (2014) Informatic parcellation of the network involved in the computation of subjective value. *Soc Cogn Affect Neurosci* 9(9):1289–1302.
5. Mars RB, et al. (2012) Connectivity-based subdivisions of the human right "temporoparietal junction area": Evidence for different areas participating in different cortical networks. *Cereb Cortex* 22(8):1894–1903.

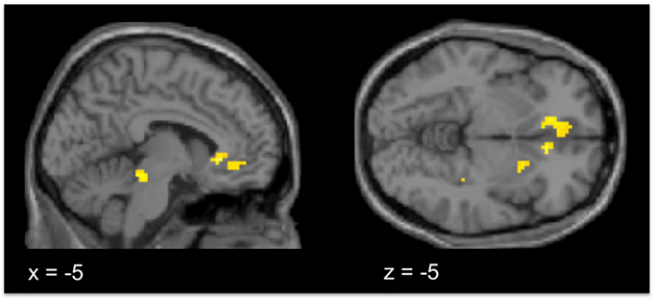

Fig. S1. Parametric modulation of activity by selfish reward magnitude after selfish decisions in the VMPFC (and the ventral striatum).

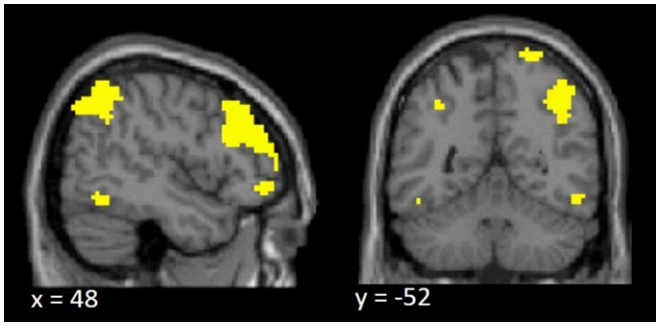

Fig. S2. Conjunction analysis of the parametric modulation of the temptation to be selfish after a generous decision and after presentation of the second option in that trial, given a generous decision. Overlap is seen especially within the boundaries of the TPJ (48, −52, 37).

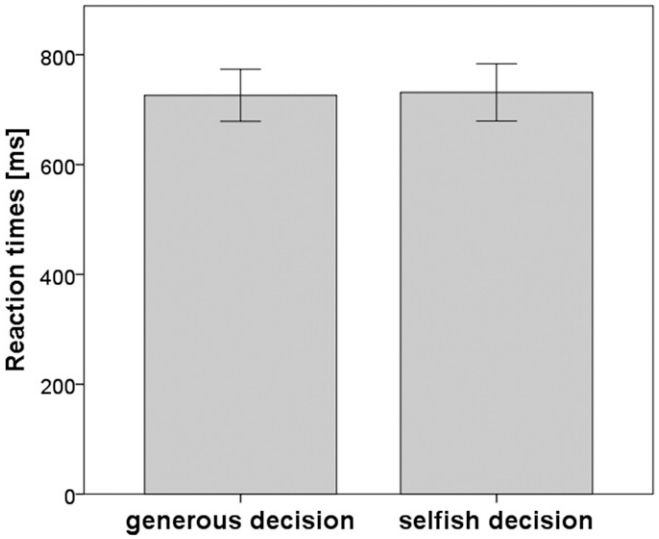

Fig. S3. Mean reaction times, split by decision. Mean reaction times were calculated first on an individual level and then summarized on a group level. Error bars indicate ±1 SE.

Table S1. GLM1: Regions showing parametric modulation by the selfish reward magnitude during selfish decisions

Region	Side	Cluster size	MNI coordinates	*t* value
Inferior frontal gyrus	R	87	27, 8, −17	4.91
Brainstem, cerebellum	R	22	−9, −28, −14	3.71
Middle temporal gyrus	R	23	57, −7, −14	3.37
Hippocampus	R	21	30, −25, −11	3.67
Anterior cingulate	R	28	9, 29, −5	3.55
Anterior cingulate	L	47	−15, 44, 4	4.03
Insula	R	17	42, −16, 7	3.69
Superior temporal gyrus	R	13	57, −61, 19	3.26
Medial frontal gyrus	R	66	15, 41, 22	4.43
Supramarginal gyrus	R	43	69, −40, 37	3.88
Supramarginal gyrus	L	12	−63, −43, 40	3.33

Threshold: $k \geq 10$ voxel, $t_{(22)} > 2.8188$, $P < 0.005$.

Table S2. GLM1: Regions showing more activity for generous vs. selfish decisions at the onset of the decision (button press)

Region	Side	Cluster size	MNI coordinates	*t* value
Positive				
Cerebellum	R	97	36, −58, −32	4.22
Occipital lobe	L	219	−12, −103, −5	5.48
Inferior frontal cortex	R	241	45, 44, −17	4.64
Medial frontal cortex	R/L	28	0, 47, −20	4.21
Occipital lobe, cuneus	R/L	390	24, −100, 13	4.67
Fusiform gyrus	R	14	51, −61, −14	3.24
Middle frontal gyrus	L	161	−39, 53, 1	4.25
Inferior frontal gyrus	L	49	−33, 23, −2	3.45
Insula	R	17	42, −7, 7	3.42
Caudate	R	21	12, 8, 13	3.58
Middle frontal gyrus	R	113	36, 35, 16	4.22
Anterior cingulate	L	25	−6, 44, 13	3.28
Superior frontal gyrus	L	282	−15, 59, 22	5.44
Middle frontal gyrus	R	116	30, 5, 43	4.41
Limbic lobe, cingulate cortex	R/L	431	3, −10, 28	5.87
Anterior cingulate	R	40	6, 47, 22	4.04
Inferior parietal lobule, angular gyrus	R	690	60, −58, 31	5.11
Supramarginal gyrus	R	16	48, −19, 28	3.05
Inferior parietal lobe	L	486	−24, −79, 52	4.49
Middle frontal gyrus	L	328	−42, 20, 43	4.71
	R	15	39, 20, 37	3.29
Superior frontal gyrus	R	21	18, 32, 52	3.31
Precentral gyrus	R	26	18, −25, 61	4.04
Negative				
Temporal lobe	R	24	24, −46, 10	3.92

Threshold: $k \geq 10$ voxel, $t_{(22)} > 2.8188$, $P < 0.005$.

Table S3. GLM1: Regions showing parametric modulation by the econometrically reconstructed ORU during generous decisions

Region	Side	Cluster size	MNI coordinates	*t* value
Rolandic operculum	L	69	−42, −19, 19	4.65
Precentral gyrus	R	21	15, −19, 64	3.80
Precentral gyrus	L	10	−18, −19, 67	3.38
Postcentral lobe	R	10	24, −31, 82	3.56

Threshold: $k \geq 10$ voxel, $t_{(22)} > 2.8188$, $P < 0.005$.

Table S4. GLM2: Regions showing parametric modulation by the difference between own-reward value and ORU (i.e., the temptation to choose the selfish option) at decision onset, given a generous choice

Region	Side	BA	MNI coordinates	*t* value
Cerebellum	R	10	27, −67, −32	4.16
Superior temporal gyrus	L	10	−33, 20, −29	3.53
Brainstem, cerebellum	R	18	6, −31, −23	4.33
Occipital lobe	L	186	−48, −64, −14	4.78
Inferior frontal gyrus	R	185	30, 20, −14	5.19
Inferior temporal lobe	R	34	51, −58, −14	3.73
Occipital lobe	R	37	30, −88, −5	3.52
Middle frontal gyrus	R	475	51, 41, 25	5.65
Middle orbitofrontal lobe	L	15	−48, 47, −5	3.55
Medial frontal gyrus	R/L	924	9, 23, 34	5.38
Occipital lobe	L	58	−33, −94, 16	4.50
	R	13	33, −85, 10	3.16
Posterior cingulate	R	24	9, −61, 13	3.43
Middle frontal gyrus	L	37	−21, 62, 25	3.44
Superior medial frontal	R	10	12, 68, 22	3.12
Middle frontal gyrus	L	117	−51, 17, 34	4.37
Inferior parietal lobule,	R	309	42, −79, 46	5.98
angular gyrus			42, 0.49, 46	4.23
			54, −61, 43	4.20
Precentral	L	14	−42, 2, 43	4.01
Inferior parietal lobule	L	32	−36, −49, 43	3.57

Threshold: $k \geq 10$ voxel, $t_{(22)} > 2.8188$, $P < 0.005$.

Table S5. GLM2: Regions showing stronger parametric modulation by the difference in own-reward value and ORU during generous than selfish decisions

Region	Side	Cluster size	MNI coordinates	*t* value
Positive				
Cerebellum	R	19	36, −58, −41	3.37
	L	19	−6, −85, −32	3.25
Occipital lobe	L	677	−33, −97, 16	5.13
Inferior temporal lobe	R	103	54, −43, −14	4.77
Inferior frontal gyrus	R	244	33, 26, −5	6.26
	L	117	−33, 20, 4	5.28
Middle occipital gyrus	R	319	36, −91, −8	4.76
Superior frontal gyrus	R/L	2,190	51, 44, 25	6.98
Occipital lobe	R	20	36, −70, −8	4.15
Cuneus	L	14	−12, −76, 10	3.26
Superior medial frontal	L	16	−6, 50, 19	3.21
Middle frontal gyrus	L	345	−51, 23, 34	5.26
Precuneus	R	114	6, −67, 40	3.53
Parietal lobe, angular gyrus	R	547	42, −79, 46	7.09
Parietal lobe	L	167	−33, −52, 43	5.01
Negative				
Temporal lobe	R	83	36, −37, −8	3.96
Frontal lobe	L	372	−21, −4, 28	5.03
Frontal lobe	R	72	21, 35, −5	4.37
Temporal lobe	L	23	−30, −49, 1	3.92
Inferior parietal lobule	L	420	−57, −34, 22	4.91
Rolandic operculum	R	15	66, 8, 4	3.85
Supramarginal gyrus	R	318	63, −28, 31	4.50
Cerebrum	R	172	18, −1, 28	4.06
Medial frontal gyrus	R	110	9, −13, 61	4.13
Parietal lobe	R	56	18, −34, 49	3.63
Postcentral	R	313	24, −52, 76	5.75
Postcentral	L	111	−21, −49, 76	3.77

Threshold: $k \geq 10$ voxel, $t_{(22)} > 2.8188$, $P < 0.005$.

Table S6. PPI: Regions showing stronger task relevant functional connectivity with the right TPJ during generous than selfish decisions

Region	Side	Cluster size	MNI coordinates	*t* value
Cerebellum	L	15	−18, −40, −44	3.89
	L	16	−27, −34, −32	4.09
Superior temporal gyrus	L	22	−51, 17, −23	3.87
Middle temporal gyrus	R	191	57, 11, −26	4.71
Inferior frontal gyrus	L	34	−33, 20, −20	3.58
Anterior cingulate	R/L	293	−6, 32, −2	6.60
Insula	L	1,522	−36, −16, 19	5.90
	R	226	39, 11, 7	4.91
Superior temporal gyrus	R	37	72, −34, 19	4.24
Supramarginal gyrus	R	21	51, −52, 25	3.85
Cingulate gyrus	L	10	−15, −22, 25	3.89
Precuneus	L	18	−9, −55, 34	4.03
Inferior parietal lobule	R	315	69, −37, 37	7.42
Middle frontal gyrus	L	162	−27, 29, 43	4.80
Medial frontal gyrus	R	139	9, −22, 55	4.52
Precentral gyrus	L	108	−42, −22, 49	4.05

Threshold: $k \geq 10$ voxel, $t_{(14)} > 2.8188$, $P < 0.005$.